THERMOCAPILLARY FLOWS STABILITY IN FLOATING ZONE UNDER MICROGRAVITY

O. Bouizi, C. Delcarte, G. Kasperski
University Paris-Sud XI, LIMSI-CNRS, BP 133, 91403 Orsay Cedex France
Corresponding author: *delcarte@limsi.fr*

Keywords: *thermocapillary convection, floating zone, instability, spectral method*

Abstract

The first transition of axi-symmetric thermocapillary convection flows in a floating zone breaks the symmetry around its mid-plane. This is observed on a very large region of Prandtl number values. A Hopf bifurcation is observed, giving rise to oscillatory flows, except for $Pr \in [3.4\,10^{-3}, 3.15\,10^{-2}]$ where a stationary transition occurs.

1 Introduction

The floating zone is a crucible-free process used to produce high-quality crystals. A molten zone is created by a lateral heating, between a feed and a single crystal rod, and held by capillary forces. The translation of the material through the heat flux induces the solidification of the crystal. Temperature gradients induce surface tension variations which are the source of thermocapillary convection. In order to reduce buoyancy effects, experiments have been performed in a low gravity environment and have demonstrated that thermocapillary convection alone can induce defects in the product due to flow instabilities. A major goal is to identify the mechanisms leading to the growth of those instabilities. The experimental difficulty comes from the fact that measurements in the core of the flow are usually limited to transparent fluids, that is having a Prandtl number value (Pr), larger than 6 or so. However, it has been shown that, just as well in real experiments as in numerical experiences, performed on the simplified half-zone model, the transitions thresholds strongly depend on the Prandtl number value. It is thus interesting to study the nature and thresholds of the instabilities of the thermocapillary flow in a full liquid bridge as a function of the Prandtl number.

In the present contribution, we study the perturbation of the axisymmetric steady state through the 2D mode as a function of the Prandtl and Marangoni number values. Chénier et al [2] pointed out at $Pr = 0.01$ a steady 2-D transition, breaking the liquid bridge symmetry about the mid-plane, which is the basic hypothesis when the half-zone configuration is used as a model of the full zone. We will study the dependence of the threshold Marangoni values and bifurcations nature with respect to the Prandtl number value. The growth rate of the destabilizing eigenmode is analysed by an energy balance using a centrifugal formulation.

2 The model

The model consists in a vertical cylindrical liquid bridge of aspect ratio $A = H/R$, between two isothermal parallel concentric rigid disks, of radius R, separated by a distance H, at the temperature T_m. The geometrical configuration is presented in Fig.1 where $\mathbf{e}_r$ and $\mathbf{e}_z$ are the radial and axial unit vectors respectively, r and z being the corresponding coordinates. The origin O is located at the center of the full liquid bridge. The free surface is non-deformable and heated with a steady heating flux $Q(z)$ symmetric about the mid-plane defined by $z = 0$. The heat flux $Q(z)$ is equal to $Q_0\, q(z)$, with Q_0 the maximum heat

flux density and $q(z)$ the non-dimensional flux.

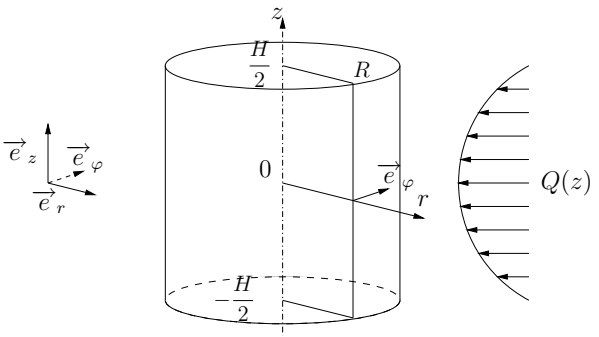

FIG. 1. Geometrical configuration of the floating zone

The length, temperature, velocity, pressure and time scales respectively are R, $\Delta T = Q_0\, R/\lambda$, $V = \kappa/R$, ρV^2 and R/V, where ρ and λ, κ are the fluid density, the thermal conductivity and the thermal diffusivity. The reduced temperature is $\Theta = (T - T_m)/\Delta T$. Then, non-dimensional parameters are introduced, the Prandtl and the Marangoni numbers defined by $Pr = \nu/\kappa$ and $Ma = -(\partial\sigma/\partial T)|_{T_m} R\Delta T/\mu\kappa$, where σ, μ and ν respectively stand for the surface tension, the dynamic and kinematic viscosities. The aspect ratio A is fixed to 2 in this study. Gravity is absent. The fluid is governed by the Navier-Stokes equations, the heat equation and the continuity equation for an incompressible fluid under the Boussinesq approximation. Those non-dimensional 2-D equations are:

$$\partial_t \mathbf{V} + (\mathbf{V}.\boldsymbol{\nabla})\mathbf{V} = -\boldsymbol{\nabla} P + Pr\Delta\mathbf{V} \quad (1)$$
$$\partial_t \Theta + \mathbf{V}.\boldsymbol{\nabla}\Theta = \Delta\Theta \quad (2)$$
$$\boldsymbol{\nabla}.\mathbf{V} = 0 \quad (3)$$

with the boundary condition on $z \pm 1$:

$$\mathbf{V} = 0, \quad \Theta = 0 \quad (4)$$

and on $r = 1$:

$$U = 0,\ \partial_r W = -Ma\partial_z\Theta,\ \partial_r\Theta = q(z) \quad (5)$$

where $\mathbf{V} = U\mathbf{e}_r + W\mathbf{e}_z$ and Θ are respectively the non-dimensional velocity and temperature. The operators are defined as follows:

$$\boldsymbol{\nabla}\bullet = \mathbf{e}_r\partial_r\bullet + \mathbf{e}_z\partial_z\bullet \quad (6)$$
$$\Delta\Theta = (1/r)\partial_r(r\partial_r\Theta) + \partial_z^2\Theta \quad (7)$$
$$\Delta\mathbf{V} = \left(\Delta U - U/r^2\right)\mathbf{e}_r + \Delta W\mathbf{e}_z \quad (8)$$
$$\boldsymbol{\nabla}.\mathbf{V} = (1/r)\partial_r(rU) + \partial_z W \quad (9)$$
$$\mathbf{V}.\boldsymbol{\nabla}\bullet = U\partial_r\bullet + W\partial_z\bullet \quad (10)$$

The shape of the heat flux is given by:

$$q(z) = \left(1 - (z)^2\right)^2 \quad (11)$$

The mathematical system is solved with a spectral collocation method on Gauss-Radau and GaussLobatto points in respectively the radial and axial directions. The steady flows are calculated with a Newton method [6]. To determine whether the flow is stable or not, we perform a linear stability analysis around the steady flow $(\mathbf{V}_0, \Theta_0)$ using an Arnoldi method [4]. Then the first eigenmodes of the steady flow are obtained. The real part of the eigenvalue cancels at the threshold Ma_c. This later is determined by linear interpolation. The linearised equations governing the perturbation $(\mathbf{v}, \theta)$ are:

$$\partial_t\mathbf{v} + (\mathbf{v}.\boldsymbol{\nabla})\mathbf{V}_0 + (\mathbf{V}_0.\boldsymbol{\nabla})\mathbf{v} = -\boldsymbol{\nabla} p + Pr\Delta\mathbf{v} \quad (12)$$

$$\partial_t\theta + \mathbf{v}.\boldsymbol{\nabla}\Theta_0 + \mathbf{V}_0.\boldsymbol{\nabla}\theta = \Delta\theta \quad (13)$$
$$\boldsymbol{\nabla}.\mathbf{v} = 0 \quad (14)$$

with the boundary condition on $z \pm 1$:

$$\mathbf{v} = 0, \quad \theta = 0 \quad (15)$$

and on $r = 1$:

$$u = 0,\ \partial_r w = -Ma\partial_z\theta,\ \partial_r\theta = 0 \quad (16)$$

where $\mathbf{v} = u\mathbf{e}_r + w\mathbf{e}_z$ and θ are respectively the non-dimensional velocity and temperature of the perturbation.

The model physical regularity assumes that at both extremities where the free surface is in contact with the fusion/solidification fronts, the supplied heat flux and the flux of the vertical momentum component must cancel. A simple

way to regularize the stress condition is to introduce a function that cancels at $z = \pm 1$, such as $f_n(z) = \left(1 - z^{2n}\right)^2$, n being a positive integer, here fixed to 13 according to the results of Chénier et al. [2, 3].

The tools used to study the transition mechanisms consist in the analysis of the kinetic and thermal energy growth rates of the perturbation. Nienhüser et al [7] proposed a formulation of the energy budget, independent of the coordinate system, based on the velocity decomposition of the perturbation, $(\mathbf{v}, \theta)$, into parallel and perpendicular components to the basic flow:

$$\mathbf{v} = \mathbf{v}_\perp + \mathbf{v}_\parallel \tag{17}$$

where

$$\mathbf{v}_\parallel = \left[\left(\mathbf{v} \cdot \mathbf{V}_0\right) \mathbf{V}_0\right] / \left\|\mathbf{V}_0^2\right\| \tag{18}$$

$$\mathbf{v}_\perp = \mathbf{v} - \mathbf{v}_\parallel \tag{19}$$

For a perturbation growth rate (i.e. eigenvalue) λ, the kinetic $\dot{E}_c$ and the thermal $\dot{E}_\theta$ growth rates express as:

$$\begin{aligned} \dot{E}_c &= -D_u + M_z \\ &\quad + I_u^2 + I_u^3 + I_u^4 + I_u^5 \\ &= \lambda \int_z \int_r \left(u^2 + w^2\right) \, r \mathrm{d}r\mathrm{d}z \end{aligned} \tag{20}$$

$$\begin{aligned} \dot{E}_\theta &= -D_\theta + I_\theta^1 + I_\theta^2 \\ &= \lambda \int_z \int_r \theta^2 \, r \mathrm{d}r\mathrm{d}z \end{aligned} \tag{21}$$

with

$$\begin{aligned} D_u = Pr \int_z \int_r \big[&\left((k/r)w\right)^2 \\ &+ \left(\partial_z u - \partial_r w\right)^2 \\ &+ \left((k/r)u\right)^2\big] \, r \mathrm{d}r\mathrm{d}z \end{aligned} \tag{22}$$

$$D_\theta = \int_r \int_z \left(\left(\partial_r \theta\right)^2 + \left(\partial_z \theta\right)^2\right) r \mathrm{d}r\mathrm{d}z \tag{23}$$

$$M_z = d_q \int_z \left(w \partial_r w\right)_{r=1} \mathrm{d}z \tag{24}$$

$$I_u^2 = -\int_z \int_r \mathbf{v}_\perp \cdot \left(\mathbf{v}_\perp \cdot \boldsymbol{\nabla}\right) \mathbf{V}_0 \, r \mathrm{d}r\mathrm{d}z \tag{25}$$

$$I_u^3 = -\int_z \int_r \mathbf{v}_\perp \cdot \left(\mathbf{v}_\parallel \cdot \boldsymbol{\nabla}\right) \mathbf{V}_0 \, r \mathrm{d}r\mathrm{d}z \tag{26}$$

$$I_u^4 = -\int_z \int_r \mathbf{v}_\parallel \cdot \left(\mathbf{v}_\perp \cdot \boldsymbol{\nabla}\right) \mathbf{V}_0 \, r \mathrm{d}r\mathrm{d}z \tag{27}$$

$$I_u^5 = -\int_z \int_r \mathbf{v}_\parallel \cdot \left(\mathbf{v}_\parallel \cdot \boldsymbol{\nabla}\right) \mathbf{V}_0 \, r \mathrm{d}r\mathrm{d}z \tag{28}$$

$$I_\theta^1 = -\int_z \int_r \theta \left(\mathbf{v}_\perp \cdot \boldsymbol{\nabla}\right) \Theta_0 \, r \mathrm{d}r\mathrm{d}z \tag{29}$$

$$I_\theta^2 = -\int_z \int_r \theta \left(\mathbf{v}_\parallel \cdot \boldsymbol{\nabla}\right) \Theta_0 \, r \mathrm{d}r\mathrm{d}z \tag{30}$$

D_u and D_θ are respectively the viscous and thermal dissipation, M_z the work of the thermocapillary stress on the free surface, I_u and I_θ the interactions between the steady state and the perturbation.

3 Results

Below the Ma_c transition threshold, the steady state of the floating zone is composed of two coun ter-rotating cells which, due to the axial symmetries of the cylindrical configuration and of the boundary conditions, are symmetric with respect to the $z = 0$ mid-plane. The radial velocity and the temperature of the steady flow are even functions with respect to z while the axial velocity is an odd function. The steady state fields, at low and high Prandtl number values, have been widely depicted by Kasperski at al [5]. At $Pr = 0.01$, the steady-state solution becomes non-symmetric via a subcritical pitchfork bifurcation, followed by a saddle-node bifurcation [2]. We have expanded the analysis over a wide range of Pr number. The threshold diagram of the floating zone and the corresponding critical frequency, in case of Hopf bifurcation, are respectively shown in Fig. 2 and in Fig. 3. At low Pr numbers, the threshold Ma_c depends linearly on the Pr. There, the critical Reynolds number $Re_c = Ma_c/Pr$ of the steady flow is rather constant. This indicates that at low Pr number, the

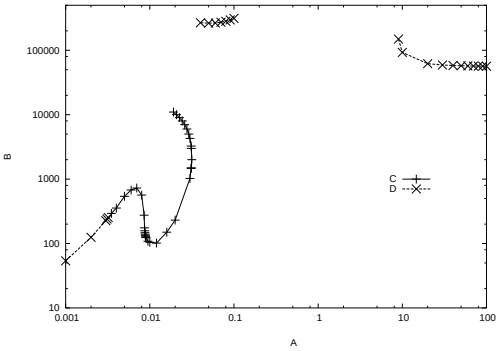

FIG. 2. Critical Ma_c value as a function of Pr number

perturbation is hydrodynamic. At high Pr numbers, the threshold $Ma_c \approx 56500$ depends no more on the Pr number, indicating that the nature of the perturbation is hydrothermal.

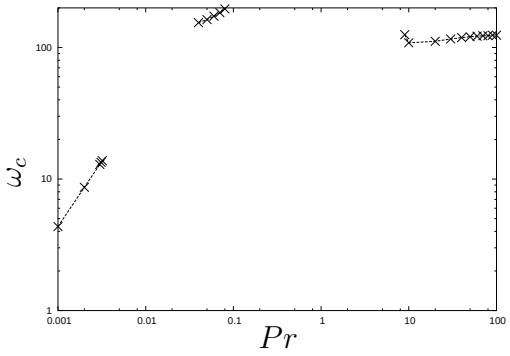

FIG. 3. Critical frequency of the Hopf bifurcation at the threshold

The bifurcation map is divided into several regions, starting from the smallest Pr values:
- $Pr \in [10^{-3}, 3.4\,10^{-3}]$: Hopf bifurcations,
- $Pr \in [3.4\,10^{-3}, 3.15\,10^{-2}]$, $Ma \lesssim 10^3$: subcritical pitchfork bifurcations,
- $Pr \in [1.9\,10^{-2}, 3.15\,10^{-2}]$, $Ma \gtrsim 10^3$: restabilizing pitchfork bifurcations (computations have not been performed below $1.9\,10^{-2}$),
- $Pr \in [4\,10^{-2}, 1\,10^{-1}]$: Hopf bifurcations,
- $Pr \in [9, 100]$: Hopf bifurcations.

Computations have not been achieved between the last two Hopf bifurcations, namely $Pr \in [1\ 10^{-1}, 9]$. Figure 4 and 5 display the stream function or the temperature of the leading destabilizing modes, in four regions. In case of Hopf bifurcation, light patches indicate the higher moduli and the phase iso-levels, normalised between –1 an 1, are solid or dot lines. Opposite signs correspond to opposite phases. In all cases, the stream functions and temperature of the leading disturbance get opposite symmetries with respect to the steady state. Consequently, the resulting bifurcations of the steady states can not be observed in the academic half-zone configuration.

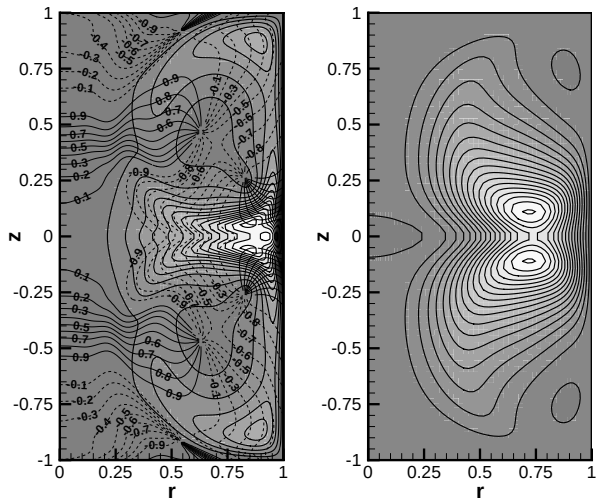

FIG. 4. Disturbance stream function at, respectively, $Pr = 0.002$, $Ma = 130$ and $Pr = 0.01$, $Ma = 106$.

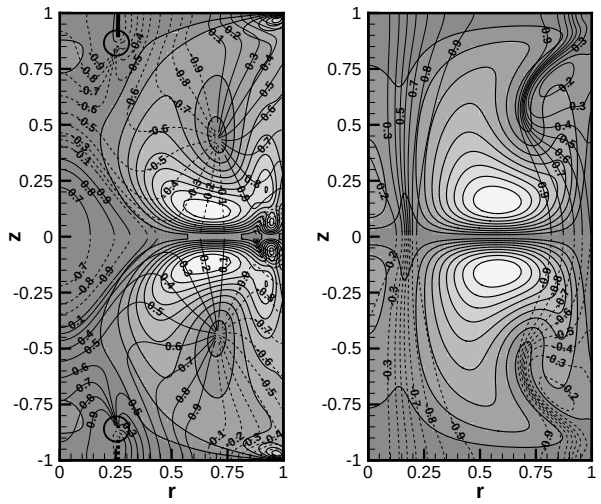

FIG. 5. Temperature iso-levels of the disturbance, at respectively, $Pr = 0.06$, $Ma = 270000$ and $Pr = 20.$, $Ma = 62100$

It has been shown by Chenier et al [2] that the stationary anti-symmetric disturbance, at $Pr = 0.01$, leads to the existence of non symmetric stable steady flows which present two counter-rotating cells of very different sizes.

In case of the here above considered Hopf bifurcations, the system $(1) - (5)$, at Marangoni number values larger that the Ma_c thresholds, were computed with the non-linear time-dependent code. The stream functions at two chosen times of the τ period are presented in Fig. 6, at $Pr = 0.002$, $Ma = 140$. The two cells alternatively growth and decrease, breaking the symmetry around the mid-plane. Despite the discrepancy in the values of the Marangoni numbers, the flow's behaviour is very similar at $Pr = 0.006$, $Ma = 280000$ (Fig. 7).

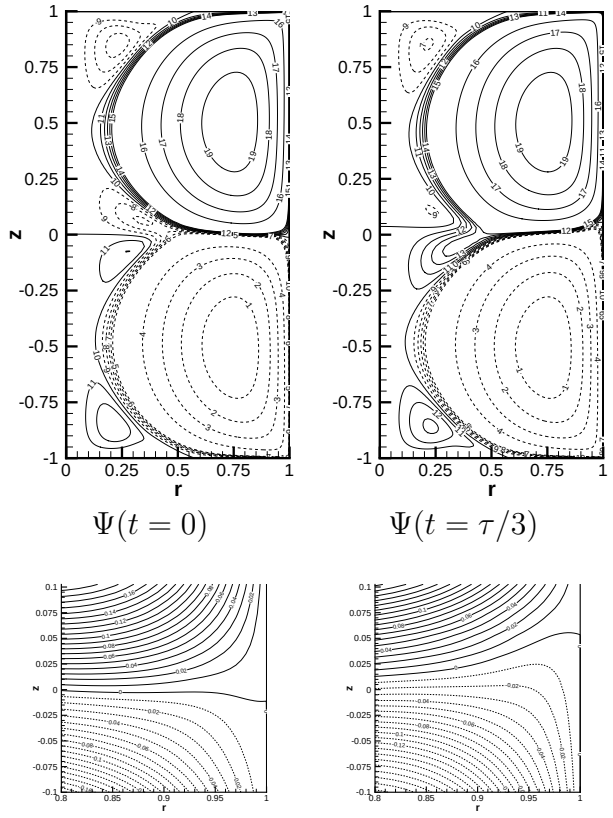

FIG. 6. Stream function at two times of a period ($t = 0$ and $t = \tau/3$ (upper panels) and corresponding details (lower panels) at $Pr = 0.002$, $Ma = 140$.

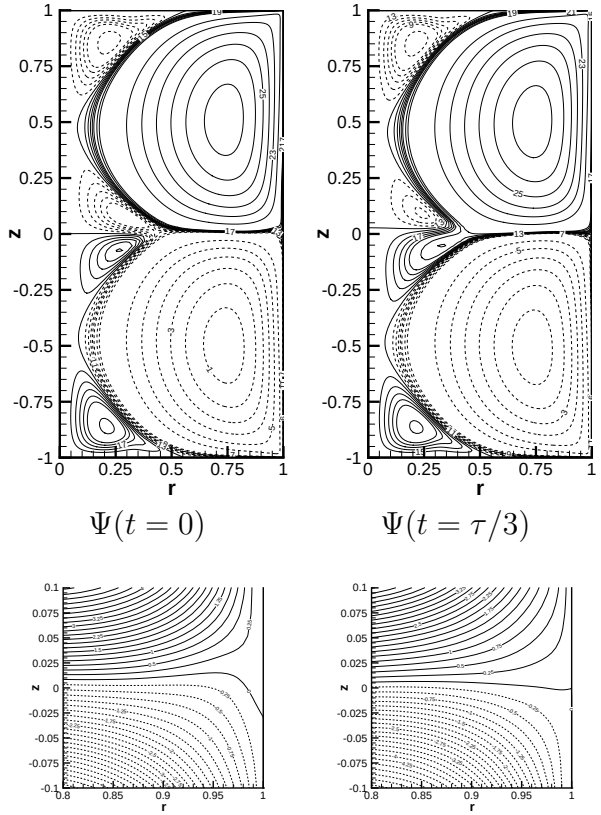

FIG. 7. Stream function at two times of a period ($t = 0$ and $t = \tau/3$ (upper panels) and corresponding details (lower panels) at $Pr = 0.06$, $Ma = 280000$.

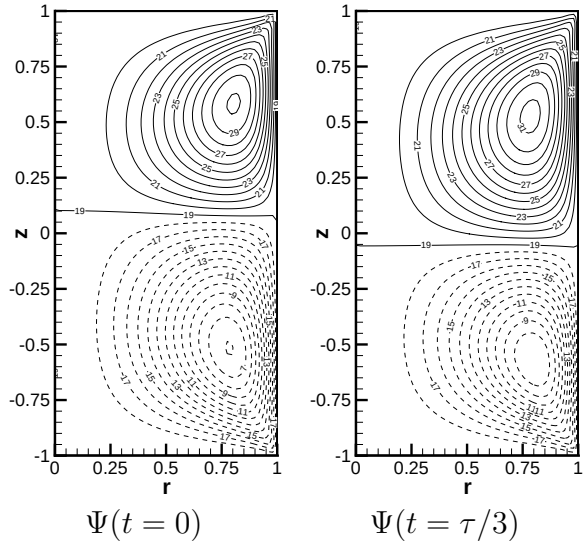

FIG. 8. Stream function at two times of a period ($t = 0$ and $t = \tau/3$); $Pr = 100$, $Ma = 60000$

At high Prandtl number values, the flow is mainly governed by momentum diffusion and its destabilization is due to thermal effects [5]. In Fig. 8 are shown the stream function contours, at two times of a period, for $Ma = 60000$ ($Ma_c = 31647$). The symmetry breaking can be viewed on the time evolution of the zero stream function line which oscillates around $z = 0$. It should be pointed out that no instability has been observed in the corresponding half zone model at that value of Pr.

The local kinetic power of the perturbation is depicted in Fig. 9, in case of transition of hydrodynamic origin. When the transition origin is thermal, the local thermal power of the perturbation is shown (Fig. 10). The values are multiplied by r and respectively normalized with the viscous dissipation $\langle D_u \rangle$ and the thermal dissipation $\langle D_\theta \rangle$. In case of Hopf bifurcations, the mean values on one period were calculated.

The spatial distributions are linked to the leading eigenmode structure. However, the comparison of Fig. 4 and 9 show that the maxima, although situated in the same regions of the (r, z) plane, can not be superposed. All are near the mid-plane. In case of the Hopf bifurcation at $Pr = 0.002$ and $Pr = 0.06$, the active zone should be near $z = 0, r = 1$. Referring to Fig. 6, in this region the upper and lower tori pulse, breaking the symmetry around the mid-plane. At $Pr = 0.01$, the destabilization mechanism was widely analysed in [2]. It was observed that the maxima loci of the perturbation stream function and local energy growth rate correspond to a region where a vorticity tongue, issued from the solid/free surface junction, is pinched between the two contra-rotative cells. The vorticity field of the steady state at $Pr = 0.002$ is given in Fig. 11. Here, also, a vorticity tongue is convected from the solid fronts towards the free surface. On the $z = 0.1$ line, the vorticity sign changes twice between $r = 0.6$ and $r = 1$. This can also be observed at $Pr = 0.06$ [1]. At high Prandtl number values, the process is quite different. As explained by Kasperski at al [5], the temperature intensifies itself alternatively in the upper and lower part of the cavity. The local energy growth rate does not throw light on this process.

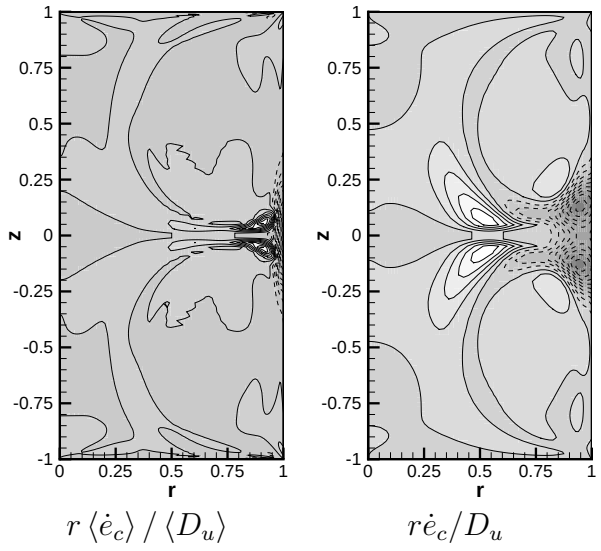

FIG. 9. Spatial distribution of the disturbance kinetic power, multiplied by r and normalized with the viscous dissipation. On the left: $Pr = 0.002$, $Ma = 130$; on the right: $Pr = 0.01$, $Ma = 106$.

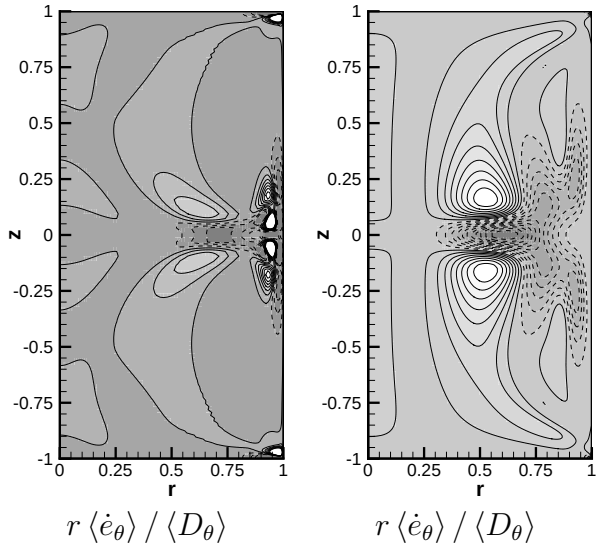

FIG. 10. Spatial distribution of the disturbance thermal power, multiplied by r and normalized with the thermal dissipation. On the left: $Pr = 0.006$, $Ma = 270000$; on the right: $Pr = 20$, $Ma = 62100$.

Following Wanschura et al [8], a deeper understanding of the destabilizing mechanisms can be obtained through the analysis of the magnitude, sign and evolution, close to the threshold, of the different terms in the energy balances. Table

1 gives, for four Pr regions, the production term ordered with respect of their absolute value; their sign, and (algebraic) evolution character as function of Ma, in the vicinity of the critical Ma_c value, are also indicated. At low (Pr, Ma) values, the destabilazing mechanism being hydrodynamic, the kinetic energy balance is considered while at high (Pr, Ma) values, due to the hydrothermal aspect of the transition, it is the thermal energy budget.

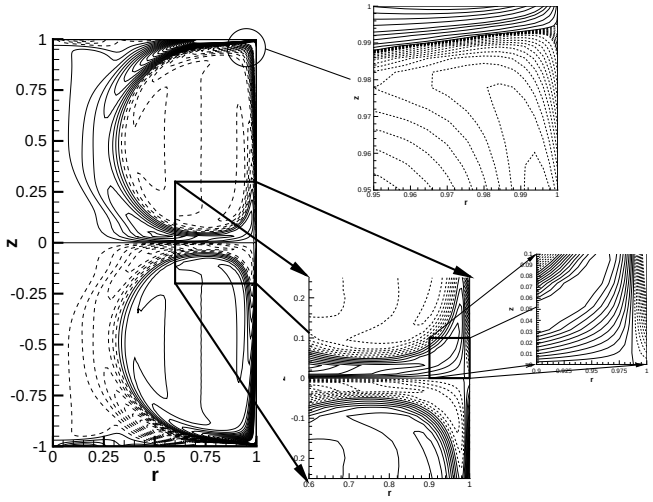

FIG. 11. Vorticity field of the steady state at $Pr = 0.002$, $Ma = 130$.

Pr				
0.002	$I_u^4+ \Uparrow$	$I_u^5- \uparrow$	$I_u^2+ \uparrow$	$I_u^3+ \uparrow$
0.01	$I_u^4+ \downarrow$	$I_u^5- \Uparrow$	$I_u^3- \sim$	$I_u^2+ \downarrow$
0.06	$I_\theta^1+ \Uparrow$	$I_\theta^2+ \downarrow$		
20	$I_\theta^1+ \Uparrow$	$I_\theta^2+ \downarrow$		

Table 1. Production dominant terms in magnitude decreasing order with sign and algebraic evolution character as a function of Ma. Double arrows ($\Uparrow$) indicate the most increasing behaviour.

In case of Hopf bifurcation, the largest term is the most growing. At $Pr = 0.002$, I_u^4 corresponds to a lift-up mechanism: there is a transport of basic-state momentum perpendicular to the base flow direction, producing energy by amplification of stream-wise perturbation. At high Pr values, the destabilazing term I_θ^1 is the rate of transfer to thermal energy from the temperature basic state to the perturbation temperature field in the direction which is perpendicular to the base flow. The stationary transition at $Pr = 0.01$ is quite different: the dominant destabilizing term is slowly decreasing and the stabilizing term I_u^5 which amplitude is half of I_u^4, is less and less negative when Ma increases. I_u^5 corresponds to a transport parallel to the base flow direction.

4 Conclusion

We have shown that the first transition type and mechanism of the axi-symmetric steady state with increasing Ma value, highly depends on the Pr values. The symmetry properties of the destabilizing mode are opposite to those of the steady base-flow giving rise to symmetry breaking. It is therefore clear that the academic half-zone is not relevant to the whole dynamics of the full zone configuration.

The energy analysis does not always provide clear information on the destabilizing mechanisms.

Acknowledgements

The authors acknowledge the IDRIS-CNRS and the CRI of University Paris-Sud for their computational ressources.

References

[1] Bouizi O, *Instabilités 3D de convection thermocapillaire en zone-flottante*, Ph.D. thesis, Université Paris-Sud XI, 2004.

[2] Chénier E, Delcarte C, Kasperski G and Labrosse G, Sensitivity of the liquid bridge hydrodynamics to local capillary contributions, *Phys. Fluids*, Vol. 14, pp. 3109–3117, 2002.

[3] Chénier E, Delcarte C, Kasperski G and Labrosse G, *Interfacial Fluid Dynamics and Transport Processes, Lecture notes in Physics*, vol. 628, chap. Thermocapillary

flows and vorticity singularity, Springer-Verlag Heidelberg, pp. 176–199, 2003.

[4] Chénier E, Delcarte C and Labrosse G, Stability of the axisymmetric buoyant-capillary flows in a laterally heated liquid bridge, *Phys. Fluids*, Vol. 11, No. 3, pp. 527–541, 1999.

[5] Kasperski G, Batoul A and Labrosse G, Up to the unsteadiness of axisymmetric thermo-capillary flows in a laterally heated liquid bridge, *Phys. Fluids*, Vol. 12, No. 1, pp. 103–119, 2000.

[6] Mamun C and Tuckerman L, Asymmetry and Hopf bifurcation in spherical Couette flow, *Phys. Fluids*, Vol. 7, No. 1, pp. 80–91, 1995.

[7] Nienhüser C and Kuhlmann H, Stability of the thermocapillary flows in non-cylindrical liquid bridges, *J. Fluid Mech.*, Vol. 458, pp. 35–73, 2002.

[8] Wanschura M, Shevtsova V, Kuhlmann H and Rath H, Convective instability mechanisms in thermocapillary liquid bridges, *Phys. Fluids*, Vol. 7, No. 5, pp. 912–925, 1995.